Computational and Theoretical Chemistry 966 (2011) 322–327

Contents lists available at ScienceDirect

Computational and Theoretical Chemistry

journal homepage: www.elsevier.com/locate/comptc

Density-functional study of the sign preference of the binding of 1-propanol to tungsten oxide seed particles

Kai Ruusuvuori *, Theo Kurtén, Ismael K. Ortega, Ville Loukonen, Martta Toivola, Markku Kulmala, Hanna Vehkamäki

Division of Atmospheric Sciences, Department of Physics, P.O. Box 64, FI-00014, University of Helsinki, Finland

ARTICLE INFO

Article history:
Received 3 December 2010
Received in revised form 16 March 2011
Accepted 19 March 2011
Available online 25 March 2011

Keywords:
Sign preference
DFT
Tungsten oxide
1-Propanol

ABSTRACT

The binding of 1-propanol to neutral and singly charged tungsten oxide seed particles was studied using quantum chemical methods. Three different density functionals and three basis sets were employed, and the results were compared with each other as well as with results previously published by other groups. Our results implicate a positive sign preference for all studied tungsten oxide species. Molecular structures obtained for pure tungsten oxide show good agreement with previous results.

1. Introduction

The motivation for this study was twofold. The first motivation was that nucleation on ions is an important process in the atmosphere. Even though the majority of atmospheric nucleation is believed to happen via neutral pathways [1,2], ion-induced nucleation may play some part, especially in regions where air ion or ion cluster concentrations are relatively high. Also, the majority of detection methods for nucleating clusters rely on charging, which makes understanding processes that involve ions vital.

Ions of opposite sign were observed to exhibit different nucleation rates as early as 1897 [3], but the reason for this sign preference remained a mystery for more than a century. In a recent paper by Nadykto et al. [4] it was demonstrated that the sign effect can be predicted by carrying out relatively simple quantum chemical calculations. This means we can use quantum chemical methods to help us understand the role of ion-induced nucleation in atmospheric conditions. Recently done calculations for sulfuric acid by Kurtén et al. [5] are another example of how quantum chemical methods can be applied to atmospheric systems. However, the computational methods in use today are generally iterative methods that employ a variety of approximations in order to keep the cost in computational resources reasonable. Because of this, theoretical predictions need to be compared with high-quality experimental results whenever possible, in order to gain reliable insight on the initial steps of ion-induced nucleation.

In this study, we have examined the sign preference of the binding of a single 1-propanol molecule to small tungsten oxide molecules with different charge. In experimental studies such as the one performed by Winkler et al. [6], tungsten oxide particle generators can be used to produce nearly monodispersed particles smaller than 2 nm in diameter. Nanoparticles such as these are valuable when studying the initial steps of nucleation. Thus, while tungsten oxide particles probably have no direct relevance to the real atmosphere, they still have an important role to play in atmospheric sciences. This brings us to the second motivation for this study: the choice of method for doing simulations is non-trivial.

While accurate simulation of transition metals, such as tungsten, generally requires the use of a very high level of theory due to the strong multireference nature of their wave functions, the computational cost for multireference methods such as multireference configuration interaction quickly becomes unfeasible as we move from single atoms and dimers to systems with a larger number of atoms. One solution to this problem is to use density functional theory (DFT), which scales more favorably with system size, and has had some success [7] in treating transition metal systems. Care has to be taken, however. In DFT calculations, the choice of density functional and basis set plays a major role, since a single density functional does not generally work equally well in every situation. Thus, the quality of results may vary greatly. This leads to a need to perform the simulations using different density functionals and basis sets, unless one can be relatively sure that the

* Corresponding author. Address: P.O. Box 64, Gustaf Hällströmin katu 2, FI-00014, University of Helsinki, Finland. Tel.: +358 (0) 9 191 50650.
E-mail address: kai.ruusuvuori@helsinki.fi (K. Ruusuvuori).

2210-271X/$ - see front matter © 2011 Elsevier B.V. All rights reserved.
doi:10.1016/j.comptc.2011.03.030

system in question is not very sensitive to the choice of theoretical method.

2. Methods

A quantum chemical study of the structure and electronic energies of WO, WO^+, WO_2, WO_2^-, WO_2^+, WO_3, WO_3^-, WO_3^+, W_3O_9, $W_3O_9^-$, $W_3O_9^+$, $(WO_2)(C_3H_8O)$, $(WO_2^-)(C_3H_8O)$, $(WO_2^+)(C_3H_8O)$, $(WO_3)(C_3H_8O)$, $(WO_3^-)(C_3H_8O)$, $(WO_3^+)(C_3H_8O)$, $(W_3O_9)(C_3H_8O)$, $(W_3O_9^-)(C_3H_8O)$ and $(W_3O_9^+)(C_3H_8O)$ was performed employing the quantum chemistry programs Spartan [8], Gaussian 03 [9], Gaussian 09 [10], SIESTA [11] and ADF [12–14] with ADF-GUI [15]. Molecular visualization programs Molden 4.6 [16] and Molekel 4.3 [17] were used to study the structures and produce the geometry figures in this study.

We worked with the assumption that the strength of the chemical bond between the seed molecule and a single 1-propanol molecule is an indicator of the sign preference. In other words, if the 1-propanol bonded more strongly to a negatively charged seed molecule than to a positively charged one, this was interpreted as implying a negative sign preference (and vice versa). For computational reasons we used single WO_2 and WO_3 molecules as seed particles, although we acknowledge that the size of the experimentally measured seed particles may have allowed dimers or even trimers. The W_3O_9 in turn corresponds to $(WO_3)_3$ and its properties are close to the bulk properties of WO_3 [18,19], providing us with a rough estimate for the bulk limit.

We also focused our attention only to the binding energies of two specific and separate molecules, and not on possible chemical reactions such as proton transfer. If such chemical reactions took place in the simulation runs, these cases were not taken into account in our final considerations. The main reason for this is that such reactions very likely can happen only for one 1-propanol molecule, and would thus not be representative for the actual heterogeneous nucleation process, where a large number of 1-propanol molecules condense onto the seed.

The quantum chemical methods used in this study were all based on density functional theory. On the SIESTA program suite, we used the semiempirical BLYP [20–22] and nonempirical RPBE [23] density functionals in the general gradient approximation (GGA) [24–26] with a DZP [27] basis set and relativistic norm-conserving pseudopotentials for the atoms. The PBE functional has been shown to give quite good lattice constants for WO_3 compared to experimental results [28], and the RPBE revision of the PBE functional has been shown to give improved results over PBE [29] in some cases. However, we did not have any conclusive data on whether the RPBE density functional would work better than the BLYP functional for our simulations or indeed if either RPBE or BLYP would perform acceptably well. Thus, we chose to use both functionals and compare the results. On the Gaussian 03 program suite we used a nonempirical meta-GGA density functional, TPSSTPSS [30,31], with two basis sets: SDD, which uses D95V [32] up to argon and Stuttgart/Dresden effective core potentials on the remainder of the periodic table [33], and def2-QZVPP [34] with a Stuttgart/Dresden effective core potential for tungsten. The TPSSTPSS functional lies on a higher rung of the "Jacob's ladder" of density functional approximations [35] than either BLYP or RPBE. This makes it in principle better, although its performance may vary depending on the specific system.

We began our study by generating initial guesses for the sole purpose of method comparison. For the single tungsten oxide molecules, initial guesses for geometry optimizations were both made by hand using the ADF-GUI and Spartan program suites, and obtained from low level (molecular mechanics) optimizations performed on some of these hand-made geometries. The geometries were then optimized using the BLYP/DZP and RPBE/DZP methods of SIESTA. Additional re-optimization was performed on the RPBE/DZP optimized geometries with the Gaussian 03 program suite using the TPSSTPSS/SDD method. Energies were taken both from the final results of the optimization runs and separate TPSSTPSS/def2-QZVPP single point calculations for the RPBE/DZP optimized geometries.

For the systems with a 1-propanol molecule and a tungsten oxide molecule, initial guesses for the geometry optimizations were obtained similarly to the single tungsten oxide molecules. The geometries were then optimized using the SIESTA RPBE/DZP method. Electronic binding energies were calculated from the energies obtained from the optimization output as well as separate single point energy calculations performed on the RPBE/DZP optimized geometries using the TPSSTPSS/def2-QZVPP method.

Finally the amount of basis set superposition error (BSSE) was probed by performing TPSSTPSS/def2-QZVPP energy calculations for the RPBE/DZP geometries for the case of 1-propanol and WO_3 with and without the counterpoise correction. Results with all the functionals were compared with each other as well as with results obtained by other groups [18,36–38] (Fig. 1, Tables 1a and b, 2a and 2b).

To study the sign preference, a new set of SIESTA RPBE/DZP optimizations was performed, where a total of eight different initial geometries were obtained using the ADF molecule builder for all charging states of WO_2 and WO_3, and a total of five different initial geometries for all charging states of W_3O_9. Frequency calculations were performed on the RPBE/DZP optimized geometries at the RPBE/DZP level to determine whether the obtained structures were local minima or transition states. Single point energies for these geometries were then calculated using the Gaussian 03 TPSSTPSS/def2-QZVPP method. The results for the obtained geometries with the largest binding energy can be seen from Fig. 2a and b, Tables 3, 4a and 4b.

The multiplicity was two for the anionic and cationic species and one for the neutral species in all cases under study.

3. Results and discussion

As can be seen from Table 1a, with the exception of a considerably larger bond angle given by the RPBE/DZP method for the negatively charged WO_2 molecule, our results for free tungsten

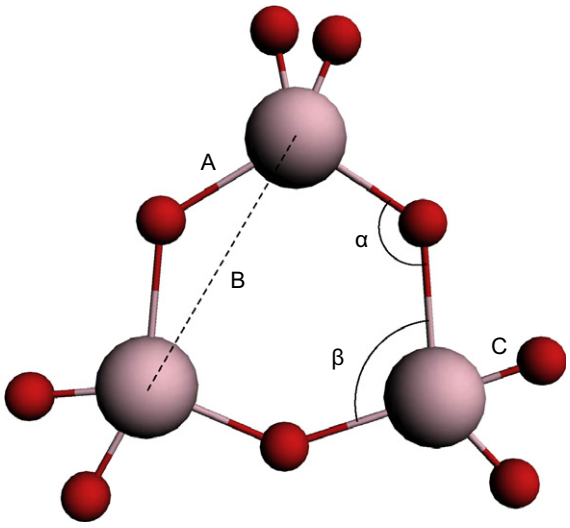

Fig. 1. A schematic of the structure of the W_3O_9 molecule. Large spheres denote tungsten atoms and small spheres oxygen atoms.

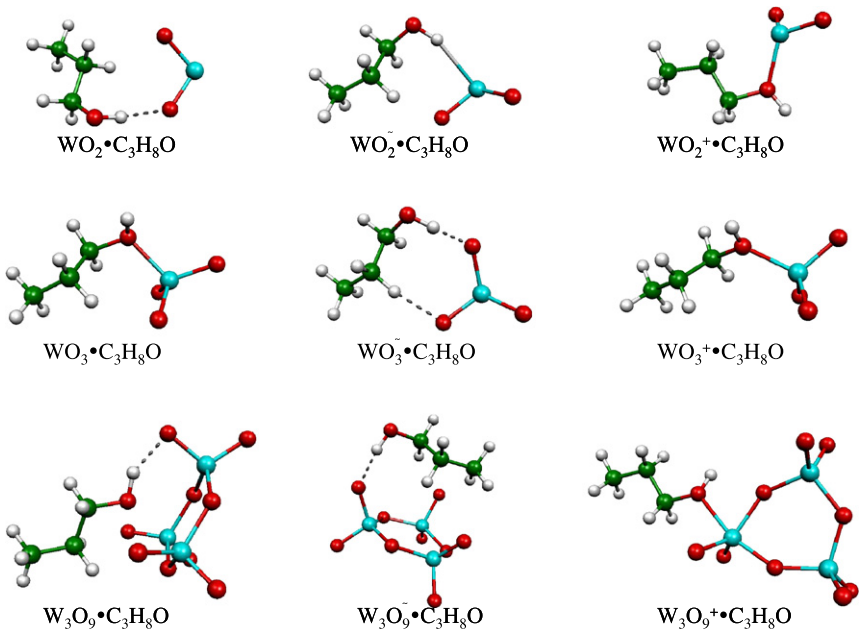

Fig. 2a. Pictures of the minimum-energy local minimum geometries listed in Table 3. Green spheres denote carbon atoms, white spheres denote hydrogen atoms, red spheres denote oxygen atoms and blue spheres denote tungsten atoms. The bonds between WO_x and 1-propanol molecules are generated by the Molden and Molekel visualization programs and may not necessarily correspond to actual covalent bonds. The lengths of these bonds or bond-like interactions are listed in Table 4a. In cases where there are more than one bond or bond-like interaction of a certain type, only the shortest length is reported.

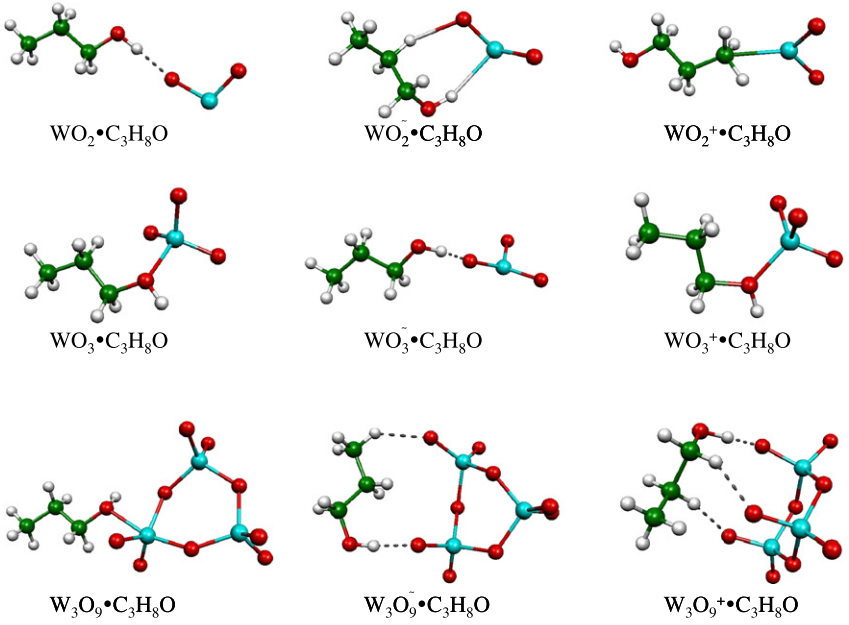

Fig. 2b. Pictures of the minimum-energy local minimum geometries with near-zero frequencies listed in Table 3. Green spheres denote carbon atoms, white spheres denote hydrogen atoms, red spheres denote oxygen atoms and blue spheres denote tungsten atoms. The bonds between WO_x and 1-propanol molecules are generated by the Molden and Molekel visualization programs and may not necessarily correspond to actual covalent bonds. The lengths of these bonds or bond-like interactions are listed in Table 4b. In cases where there are more than one bond or bond-like interaction of a certain type, only the shortest length is reported.

oxide molecules are quite similar to the results obtained by other groups using different methods. The same can be seen from Table 1b, where deviations from the results by Huang et al. remained relatively small except for the vertical detachment energy (VDE), which is the energy of the neutral molecule minus the energy of the anion (both in their ground electronic state) at the equilibrium geometry of the anion. For the VDE the BLYP/DZP and RPBE/DZP methods gave very poor results. The TPSSTPSS/SDD method of Gaussian 03 gave an overestimation of 0.47 eV when used to re-optimize the RPBE/DZP geometry whereas a single point energy calculation on the RPBE/DZP geometry with the TPSSTPSS/def2-QZVPP method resulted in an overestimation of 0.34 eV. It would thus seem that the problem is not so much in the geometry as it is in the energies given by the BLYP/DZP and RPBE/DZP methods.

Overall, based on this initial comparison it seemed that our chosen methods perform adequately for the geometry optimization. The TPSSTPSS/SDD method is computationally more demanding than the BLYP/DZP and RBE/DZP methods, but did not seem to give

Table 1a
Comparison of structures and energies with results from other groups.

Method	r_{W-O} (Å)	OWO (°)	OWOO (°)	Energy (hartree)
WO				
1*	1.6749	–	–	−142.2594359
2*	1.6641	–	–	−142.9602519
TPSS**	1.6990	–	–	−142.2244048
BLYP	1.6680	–	–	−41.2511993
RPBE	1.6586	–	–	−41.4498768
TPSS***	–	–	–	−142.2758654
WO^+				
1*	1.6594	–	–	−141.9673959
2*	1.6473	–	–	−142.6645348
TPSS**	1.6838	–	–	−141.9393052
BLYP	1.6612	–	–	−41.0178067
RPBE	1.6511	–	–	−41.2338939
TPSS***	–	–	–	−141.9951549
WO_2				
3*	1.72	103.79	–	–
4*	1.69	104.75	–	–
TPSS**	1.73	103.93	–	–
BLYP	1.70	104.62	–	–
RPBE	1.69	104.19	–	–
WO_2^-				
3*	1.76	116.44	–	–
4*	1.74	117.93	–	–
TPSS**	1.78	117.18	–	–
BLYP	1.76	118.11	–	–
RPBE	1.79	130.43	–	–
WO_3				
5*	1.807	103.8	108.1	−292.3750
6*	1.746	106.9	114.1	−293.5414
TPSS**	1.767	106.3	113.0	−292.9005
BLYP	1.753	105.3	110.9	−73.5958
RPBE	1.742	105.2	110.8	−73.8747
TPSS***	–	–	–	−293.0246

* Method 1: Gaussian 98 B3LYP/SDD for tungsten and 6–31G* for oxygen, ground state [36]; Method 2: Gaussian 98 B3LYP/LanL2DZ for tungsten and 6–31G* for oxygen, ground state[36]; Method 3: Gaussian 94 BP86/LanL2DZ[37]; Method 4: Gaussian 94 B3LYP/LanL2DZ/6–31 + G* [37]; Method 5: Gaussian 94 MP2/LanL2DZ [38]; Method 6: Gaussian 94 B3LYP/LanL2DZ [38].
** A Gaussian 03 TPSSTPSS/SDD re-optimization of the SIESTA RPBE/DZP optimized geometry.
*** G03 TPSSTPSS/def2-QZVPP single point energy calculation for the RPBE/DZP optimized geometry.

Table 1b
Comparison of structures and vertical detachment energies. A, B, C, α and β are shown in Fig. 1.

Method	A (Å)	B (Å)	C (Å)	α (°)	β (°)	VDE (eV)
W_3O_9						
1*	1.908	3.552	1.706	137.1	102.9	–
TPSS**	1.924	3.615	1.751	139.8	100.1	–
BLYP	1.924	3.525	1.732	132.8	105.9	–
RPBE	1.917	3.514	1.721	130.7	106.8	–
W_3O_9						
Exptl[17]	–	–	–	–	–	~4.2
1*	1.923	3.265	1.724	116.2	123.8	4.39
TPSS**	1.951	3.299	1.766	115.6	124.5	4.67
BLYP	1.943	3.251	1.748	113.3.	126.2	2.46
RPBE	1.934	3.215	1.738	112.4	127.4	2.66
TPSS***	–	–	–	–	–	4.54

* Method 1: NWChem 4.6 B3LYP/augmented Stuttgart 14 for tungsten and aug-cc-pVTZ for oxygen[18].
** G03 TPSSTPSS/SDD re-optimization of the SIESTA RPBE/DZP optimized geometry.
*** G03 TPSSTPSS/def2-QZVPP single point energy calculation for the RPBE/DZP optimized geometry.

any significant improvement for the optimized geometries. Since the difference between RPBE and BLYP density functionals proved in addition to be small, we decided to use the nonempirical RPBE instead of the semiempirical BLYP or the nonempirical meta-GGA TPSSTPSS for the geometry optimizations in the sign preference calculations. However, due to the VDE results, we decided to use the TPSSTPSS/def2-QZVPP method for the energies by performing single point energy calculations on the RPBE/DZP optimized geometries.

Table 2a
Comparison of binding energies given by the RPBE/DZP and TPSSTPSS/def2-QZVPP methods for a set of test geometries. The RPBE binding energies were calculated from the energies calculated by SIESTA during the RPBE/DZP optimization runs. The TPSSTPSS binding energies were calculated from single point energies calculated at the TPSSTPSS/def2-QZVPP level for the RPBE/DZP optimized geometries. These structures were not used for the actual sign preference calculations.

	ΔE_{elec} (kcal/mol)	
	RPBE	TPSSTPSS
$WO_2.C_3H_8O$	−13.0	0.5
$WO_2.C_3H_8O$	−45.6	−8.6
$WO_2^+.C_3H_8O$	−19.9	−3.0
$WO_3.C_3H_8O$	−16.4	7.9
$WO_3.C_3H_8O$	−40.0	−10.3
$WO_3^+.C_3H_8O$	−52.7	−50.5
$W_3O_9.C_3H_8O$	−19.8	3.0
$W_3O_9.C_3H_8O$	−31.4	−1.3
$W_3O_9^+.C_3H_8O$	−49.0	−38.6

Table 2b
Binding energies calculated from TPSSTPSS/def2-QZVPP single point energy calculations performed on RPBE/DZP optimized test geometries. The single point energy calculations were performed with and without the counterpoise correction. These structures were not used for the actual sign preference calculations.

	ΔE_{elec} (kcal/mol)	
	TPSSTPSS	TPSSTPSS + counterpoise
$WO_3.C_3H_8O$	7.9	7.6
$WO_3.C_3H_8O$	−10.3	−9.8
$WO_3^+.C_3H_8O$	−50.5	−51.6

The computational results presented in Table 2a show initial test results for binding energies between 1-propanol and three different tungsten oxide seed molecules. The main purpose of these binding energies was to study the differences between the RPBE/DZP and TPSSTPSS/def2-QZVPP methods. For the RPBE/DZP method, these results imply a negative sign preference for WO_2 and a positive sign preference for WO_3 and W_3O_9. Using the TPSSTPSS/def2-QZVPP method for the energies resulted in significant quantitative change of the binding energies compared to RPBE/DZP, especially for the negatively charged cases. Together with the VDE results this could indicate that the negatively charged cases cause problems for the energy calculations of the RPBE/DZP method. This would not be totally unexpected since Kohn–Sham density functional theory has known issues with describing anions [39]. The qualitative sign preference did not change, however, but the fact that the binding energy changed sign for the uncharged cases of WO_2, WO_3 and W_3O_9 would suggest that at least the uncharged geometries were not ideal.

The counterpoise corrected binding energies for the case of 1-propanol and WO_3 presented in Table 2b show differences between 0.3 kcal/mol and 1.1 kcal/mol compared with the results without counterpoise correction. The resulting changes in the differences between charging states were not enough to affect the qualitative results. Thus, BSSE was deemed being of little importance for the cases under study.

The results for the actual sign preference calculations are presented in Table 3. Binding energies for the most strongly bound structures for each case are reported. For some structures the SIES-

Table 3
Binding energies of the most strongly bound structures. The energies were obtained from Gaussian 03 TPSSTPSS/def2-QZVPP single point energy calculations performed on geometries from SIESTA RPBE/DZP optimization runs, except for the case of $(W_3O_9^+)(C_3H_8O)$, where the single point energy calculation was performed on a TPSSTPSS/def2-QZVPP level with Gaussian 09. Initial geometries were built by hand with ADF. All listed cases are local minima, but structures which had near-zero frequencies are listed separately.

	Local minimum	Local minimum with near-zero frequencies	
	ΔE_{elec} (kcal/mol)	ΔE_{elec} (kcal/mol)	Lowest frequency (cm^{-1})
$WO_2.C_3H_8O$	−0.2	−1.5	−0.08
$WO_2^-.C_3H_8O$	−11.8	−11.9	−0.04
$WO_2^+.C_3H_8O$	−71.7	−32.7	0.10
$WO_3.C_3H_8O$	−45.7	−46.0	−0.06
$WO_3^-.C_3H_8O$	−10.9	−11.3	0.06
$WO_3^+.C_3H_8O$	−79.1	−80.1	−0.06
$W_3O_9.C_3H_8O$	−13.0	−19.8	0.04
$W_3O_9^-.C_3H_8O$	−1.3*	3.7	0.05
$W_3O_9^+.C_3H_8O$	−38.2**	−40.1	0.07

* The structure was originally generated for the method comparison.
** The structure was obtained by re-optimizing the optimized local minimum geometry of $W_3O_9.C_3H_8O$ with the charge set to +1.

TA vibrational frequency calculations gave near-zero frequencies and we have listed these structures as well as their lowest vibrational frequencies separately. For actual transition states we would expect to see clearly negative vibrational frequencies of about $-100\ cm^{-1}$ or even $-1000\ cm^{-1}$ when using SIESTA. Thus, the structures with near-zero frequencies are local minima as well and because we are not calculating thermodynamic properties, the frequencies do not present a problem. As can be seen, most of the binding energies of the structures with near-zero vibrational frequencies are very close to the local minima structures with positive lowest vibrational frequencies, except for the case of $(W_3O_9)(C_3H_8O)$, where the structure with near-zero lowest vibrational frequency is almost 6.8 kcal/mol more strongly bound, and the case of $(WO_2^+)(C_3H_8O)$, where both binding energy and the geometry of the optimized structure imply that the structure is not a very good local minimum. Another noteworthy case is $(W_3O_9^-)(C_3H_8O)$, for which the structure generated for the method testing was more strongly bound than any of the optimized structures resulting from the initial guesses generated for the study of sign preference.

We have presented pictures of the most strongly bound geometries according to our results in Fig. 2a (local minima) and Fig. 2b (local minima with near-zero vibrational frequency) and provided the .xyz-files for all listed cases as supplementary material. From Fig. 2a and 2b it can be seen that the binding of 1-propanol to a WO_x seed molecule seems to happen mostly either via the OH O atom to a WO_x W atom, or via the OH H atom to a WO_x O atom. Since O is more electronegative than H, one would assume that the former always happens for positive seeds and the latter for negative seeds, with neutrals going either way. The only case where this was not true was for $(W_3O_9^+)(C_3H_8O)$. Since the optimized structure of $(W_3O_9)(C_3H_8O)$ with near-zero lowest vibrational frequency exhibited an O···W bond, we used this structure as the geometry for a positively charged system and checked whether this would yield a minimum energy structure for $(W_3O_9^+)(C_3H_8O)$ with an O···W bond. Simply performing a single point energy calculation on the "new" positively charged structure did not yield a minimum energy structure. However, a re-optimization of the $(W_3O_9)(C_3H_8O)$ structure with charge set to +1, followed by a TPSSTPSS/def2-QZVPP single point energy calculation, resulted in a minimum energy structure with non-zero lowest vibrational frequency. Due to technical reasons the single point calculations for this one case were performed with Gaussian 09. Four additional single point calculations for different cases were performed with Gaussian 09 to insure that the choice between Gaussian 09 and Gaussian 03 did not affect the results. The resulting differences in single point energies were zero in three cases and 0.0000000040 hartree in one case.

For all three tungsten oxide seed particle species, the implied sign preference obtained with Gaussian 03 is positive. The oxidation state of tungsten seems to have an effect on the relative ordering of the negatively charged and uncharged cases, but the reason for this remains unclear. It is worth noting that the experimental sign preference results of Winkler et al. showed a negative sign preference for heterogeneous nucleation of n-propanol gas on WO_x seed particles. The most obvious candidate for this discrepancy is technical reasons. Systems with multiple heavy atoms, especially those including very heavy atoms such as tungsten, cannot in practice be treated using a high level calculation such as coupled cluster or multireference configuration interaction. For

Table 4a
Bond lengths between 1-propanol and WO_x molecules for the local minimum geometries in Fig. 2a. The first atom in bond type refers to an atom belonging to the 1-propanol and the second atom refers to an atom belonging to the WO_x molecule.

	$WO_2.C_3H_8O$	$WO_2.C_3H_8O$	$WO_2^+.C_3H_8O$	$WO_3.C_3H_8O$	$WO_3.C_3H_8O$	$WO_3^+.C_3H_8O$	$W_3O_9.C_3H_8O$	$W_3O_9.C_3H_8O$	$W_3O_9^+.C_3H_8O$
Bond type	H–O	H–W H–O	O–W	O–W	H–O	O–W	H–O	H–O	O–W
Bond length (Å)	1.91190	2.45766 2.31597	2.10200	2.11427	1.57440*	2.05608	1.81980	1.77829	2.17119

* Only the shorter of the two H–O bonds or bond-like interactions shown in Fig. 2a is given.

Table 4b
Bond lengths between 1-propanol and WO_x molecules for the local minimum geometries with near-zero frequencies in Fig. 2b. The first atom in bond type refers to an atom belonging to the 1-propanol and the second atom refers to an atom belonging to the WO_x molecule.

	$WO_2.C_3H_8O$	$WO_2.C_3H_8O$	$WO_2^+.C_3H_8O$	$WO_3.C_3H_8O$	$WO_3.C_3H_8O$	$WO_3^+.C_3H_8O$	$W_3O_9.C_3H_8O$	$W_3O_9.C_3H_8O$	$W_3O_9^+.C_3H_8O$
Bond type	H–O	H–W H–O	C–W	O–W	H–O	O–W	O–W	H–O	H–O
Bond length (Å)	1.86501	2.47425 2.33758	2.38126	2.12080	1.51222	2.06623	2.24340	1.75083*	1.39942**

* Only the shorter of the two H–O bonds or bond-like interactions shown in Fig. 2b is given.
** Only the shortest of the three H–O bonds or bond-like interactions shown in Fig. 2b is given.

this reason, less accurate methods such as DFT, with known issues with transition metals and dispersion, must be used. Even though the methods we used yielded similar results with results obtained by other groups for the free tungsten oxide molecules and clusters, introducing bonding with 1-propanol into the picture may have changed how well the methods perform. However, there seems to be at least some consistency in the modelled sign preference results. Also, the qualitative result of the strongest bond being between the positively charged tungsten oxide seed molecules and 1-propanol seems so clear that it would take more than a few minor corrections to change it. This leads us to believe that the qualitative results are quite robust, and that the more likely reason for the discrepancy lies in the differences between our idealized two-molecule simulation and the actual experiment. Further support for this belief is provided by the fact that in our simulations there were a few cases where Siesta's RPB/DZP showed a proton transfer between the 1-propanol and the tungsten oxide. These were, per our initial plan, not taken into account in our sign preference results, but still imply the existence of chemical reactions that might also affect the sign preference and may have taken place in the experiment. Furthermore, since the focus of Winkler et al. was to measure very small charged and neutral seed particles and not the chemical composition of these seed particles, the effect of possible contaminations on the seed particle composition is unknown. This also applies to possible chemical reactions during transport from the particle generator to the mixing chamber, where the actual nucleation took place.

4. Conclusions

We have performed a quantum chemical study of the optimized geometries and energies of several tungsten oxide species using the methods BLYP/DZP, RPBE/DZP and TPSSTPSS/SDD for both geometry optimizations and energies. For the energies, a combined method of RPBE/DZP optimization and TPSSTPSS/def2-QZVPP single point energy calculations was also used. The results were compared with each other and results obtained previously by other groups and overall the agreement was quite good. Furthermore, we performed a quantum chemical study concerning the sign preference of the binding of 1-propanol to three tungsten oxide species using a combined method of RPBE/DZP optimization and TPSSTPSS/def2-QZVPP single point energy calculations. Our results imply a positive sign preference for WO_2, WO_3 and W_3O_9. The experimentally observed sign preference for WO_x seed particles is negative. While technical reasons cannot be ruled out as the source of this discrepancy, the more likely sources are the differences between our idealized study and the actual experimental conditions.

Acknowledgment

We thank the CSC – IT Center for Science Ltd. for computer time and technical assistance. The financial support by the Academy of Finland Centre of Excellence program (Project No. 1118615), the Research Foundation of the University of Helsinki and ERC StG 257360-MOCAPAF is gratefully acknowledged.

Appendix A. Supplementary material

Supplementary data associated with this article can be found, in the online version, at doi:10.1016/j.comptc.2011.03.030.

References

[1] M. Kulmala, I. Riipinen, M. Sipilä, H.E. Manninen, T. Petäjä, H. Junninen, M. Dal Maso, G. Mordas, A. Mirme, M. Vana, A. Hirsikko, L. Laakso, R.M. Harrison, I. Hanson, C. Leung, K.E.J. Lehtinen, V.-M. Kerminen, Science 318 (2007) 89–92.
[2] S. Mirme, A. Mirme, A. Minikin, A. Petzold, U. Hõrrak, V.-M. Kerminen, M. Kulmala, Atmos. Chem. Phys. 10 (2010) 437–451.
[3] C.T.R. Wilson, Phil. Trans. R. Soc. A 189 (1897) 265.
[4] A.B. Nadykto, A.A. Natsheh, F. Yu, K.V. Mikkelsen, J. Ruuskanen, Phys. Rev. Lett. 96 (2006) 125701.
[5] T. Kurtén, I.K. Ortega, H. Vehkamäki, J. Mol. Struct.: THEOCHEM 901 (2009) 169–173.
[6] P.M. Winkler, G. Steiner, A. Vrtala, H. Vehkamäki, M. Noppel, K.E.J. Lehtinen, G.P. Reischl, P.E. Wagner, M. Kulmala, Science 319 (2008) 1374.
[7] F. Furche, J.P. Perdew, J. Chem. Phys. 124 (2006) 044103.
[8] Wavefunction, Inc.: Spartan '06 Windows, Wavefunction, Inc. Irvine, CA, USA, <http://www.wavefun.com>, (2006).
[9] M.J. Frisch, G.W. Trucks, H.B. Schlegel, G.E. Scuseria, M.A. Robb, J.R. Cheeseman, J.A. Montgomery, Jr., T. Vreven, K.N. Kudin, J.C. Burant, J.M. Millam, S.S. Iyengar, J. Tomasi, V. Barone, B. Mennucci, M. Cossi, G. Scalmani, N. Rega, G.A. Petersson, H. Nakatsuji, M. Hada, M. Ehara, K. Toyota, R. Fukuda, J. Hasegawa, M. Ishida, T. Nakajima, Y. Honda, O. Kitao, H. Nakai, M. Klene, X. Li, J.E. Knox, H.P. Hratchian, J.B. Cross, V. Bakken, C. Adamo, J. Jaramillo, R. Gomperts, R.E. Stratmann, O. Yazyev, A.J. Austin, R. Cammi, C. Pomelli, J.W. Ochterski, P.Y. Ayala, K. Morokuma, G.A. Voth, P. Salvador, J.J. Dannenberg, V.G. Zakrzewski, S. Dapprich, A.D. Daniels, M.C. Strain, O. Farkas, D.K. Malick, A.D. Rabuck, K. Raghavachari, J.B. Foresman, J.V. Ortiz, Q. Cui, A.G. Baboul, S. Clifford, J. Cioslowski, B.B. Stefanov, G. Liu, A. Liashenko, P. Piskorz, I. Komaromi, R.L. Martin, D.J. Fox, T. Keith, M.A. Al-Laham, C.Y. Peng, A. Nanayakkara, M. Challacombe, P.M.W. Gill, B. Johnson, W. Chen, M.W. Wong, C. Gonzalez, J.A. Pople, "GAUSSIAN 03, Revision C.02", Gaussian, Inc., Wallingford, CT, 2004
[10] M.J. Frisch, G.W. Trucks, H.B. Schlegel, G.E. Scuseria, M.A. Robb, J.R. Cheeseman, G. Scalmani, V. Barone, B. Mennucci, G.A. Petersson, H. Nakatsuji, M. Caricato, X. Li, H.P. Hratchian, A.F. Izmaylov, J. Bloino, G. Zheng, J.L. Sonnenberg, M. Hada, M. Ehara, K. Toyota, R. Fukuda, J. Hasegawa, M. Ishida, T. Nakajima, Y. Honda, O. Kitao, H. Nakai, T. Vreven, J.A. Montgomery, Jr., J.E. Peralta, F. Ogliaro, M. Bearpark, J.J. Heyd, E. Brothers, K.N. Kudin, V.N. Staroverov, R. Kobayashi, J. Normand, K. Raghavachari, A. Rendell, J.C. Burant, S.S. Iyengar, J. Tomasi, M. Cossi, N. Rega, J.M. Millam, M. Klene, J.E. Knox, J.B. Cross, V. Bakken, C. Adamo, J. Jaramillo, R. Gomperts, R.E. Stratmann, O. Yazyev, A.J. Austin, R. Cammi, C. Pomelli, J.W. Ochterski, R.L. Martin, K. Morokuma, V.G. Zakrzewski, G.A. Voth, P. Salvador, J.J. Dannenberg, S. Dapprich, A.D. Daniels, Ö. Farkas, J.B. Foresman, J.V. Ortiz, J. Cioslowski, and D.J. Fox,"Gaussian 09, Revision A.1", Gaussian, Inc., Wallingford CT, 2009
[11] J.M. Soler, E. Artacho, J.D. Gale, A. García, J. Junquera, P. Ordejón, D. Sánchez-Portal, J. Phys. Condens. Matt. 14 (2002) 2745.
[12] G. te Velde, F.M. Bickelhaupt, S.J.A. van Gisbergen, C. Fonseca Guerra, E.J. Baerends, J.G. Snijders, T. Ziegler, J. Comput. Chem. 22 (2001) 931.
[13] C. Fonseca Guerra, J.G. Snijders, G. te Velde, E.J. Baerends, Theor. Chem. Acc. 99 (1998) 391.
[14] ADF2009.01, SCM, Theoretical Chemistry, Vrije Universiteit, Amsterdam, The Netherlands, <http://www.scm.com>.
[15] ADF-GUI 2009.01, SCM, Amsterdam.
[16] G. Schaftenaar, J.H. Noordik, J. Comput.-Aided Mol. Des. 14 (2000) 123–134.
[17] P. Flükiger, H.L. Lüthi, S. Portmann, J. Weber, MOLEKEL 4.3, Swiss Center for Scientific Computing, Manno, Switzerland (2002).
[18] X. Huang, Z. Hua-Jin, L. Jun, W. Lai-Sheng, J. Phys. Chem. A. 110 (2006) 85–92.
[19] Q. Sun, B.K. Rao, P. Jena, D. Stolcic, Y.D. Kim, G. Gantefor, A.W. Castleman Jr., J. Chem. Phys. 121 (19) (2004) 15.
[20] A.D. Becke, Phys. Rev. A 38 (1988) 3098.
[21] C. Lee, W. Yang, R.G. Parr, Phys. Rev. B 37 (1988) 785.
[22] B. Miehlich, A. Savin, H. Stoll, H. Preuss, Chem. Phys. Lett. 157 (1989) 200.
[23] B. Hammer, L.B. Hansen, J.K. Norskov, Phys. Rev. B 59 (1999) 7413.
[24] J.P. Perdew, Y. Wang, Phys. Rev. B 33 (1986) 8800.
[25] J.P. Perdew, K. Burke, Y. Wang, Phys. Rev. B 54 (1996) 16533.
[26] J.P. Perdew, K. Burke, M. Ernzerhof, Phys. Rev. Lett. 77 (1996) 3865; 78 (1997) 1396(E).
[27] T.H. Dunning, J. Chem. Phys. 55 (1971) 716.
[28] C. Lambert-Mauriat, V. Oison, J. Phys.: Condens. Matter 18 (2006) 7361–7371.
[29] A. Matveev, M. Staufer, M. Mayer, N. Rösch, Int. J. Quant. Chem. 75 (1999) 865–873.
[30] J. Tao, J.P. Perdew, V.N. Staroverov, G.E. Scuseria, Phys. Rev. Lett. 91 (2003) 146401.
[31] V.N. Staroverov, G.E. Scuseria, J. Tao, J.P. Perdew, J. Chem. Phys. 119 (2003) 12129.
[32] T.H. Dunning Jr, P.J. Hay, in: H.F. Schaefer III (Ed.), Modern Theoretical Chemistry, Vol. 3, Plenum, New York, 1976, pp. 1–28.
[33] D. Andrae, U. Haeussermann, M. Dolg, H. Stoll, H. Preuss, Theor. Chim. Acta 77 (1990) 123–141.
[34] F. Weigend, R. Ahlrichs, Phys. Chem. Chem. Phys. 7 (2005) 3297.
[35] J.P. Perdew, A. Ruzsinszky, J. Tao, V.N. Staroverov, G.E. Scuseria, G.I. Csonka, J. Chem. Phys. 123 (2005) 062201.
[36] V. Blagojevic, G.K. Koyanagi, V.V. Lavrov, G. Orlova, D.K. Bohme, Chem Phys Lett 389 (2004) 303–308.
[37] G.E. Davico, R.L. Schwartz, T.M. Ramond, W.C. Lineberger, J. Phys. Chem. A 103 (1999) 6167–6172.
[38] A.C. Tsipis, C.A. Tsipis, J. Phys. Chem. A 104 (2000) 859–865.
[39] F. Jensen, J. Chem. Theory Comput. 6 (2010) 2726–2735.